JOURNAL OF SOLID STATE CHEMISTRY 69, 369–375 (1987)

Investigation of Energy Transfer Processes in Nb-Compensated $CaMoO_4 : Nd^{3+}$ Crystals

BRAHIM ELOUADI,* RICHARD C. POWELL, AND SMITH L. HOLT

Department of Physics, Oklahoma State University, Stillwater, Oklahoma 74078-0444

Received August 5, 1986; in revised form December 8, 1986

The temperature dependence and time evolution of the fluorescence was studied for samples of $CaMoO_4 : YNbO_4$ and $CaMoO_4 : NdNbO_4$, and the results are used to characterize the thermal quenching and host-sensitized energy transfer properties of these materials. Doping with $YNbO_4$ is found to enhance the room-temperature luminescence yield of $CaMoO_4$. Efficient host-sensitized energy transfer to Nd^{3+} ions was observed in $CaMoO_4 : NdNbO_4$, and the fluorescence lifetime of Nd^{3+} was found to be close to its radiative lifetime in this host.

I. Introduction

Molybdates are interesting materials for phosphor and laser applications. $CaMoO_4$ exhibits a green fluorescence emission band attributed to charge transfer transitions of the MoO_4^{2-} molecular ion (*1–3*). This is an intense luminescence at low temperatures but is strongly quenched at room temperature. Molybdates such as $CaMoO_4$ and $SrMoO_4$ doped with Nd^{3+} and charge compensated with Nb (*5*) have been shown to be good laser materials (*4–6*). We report here an investigation of the properties of thermal quenching and host-sensitized energy transfer in the materials $CaMoO_4 : YNbO_4$ and $CaMoO_4 : NdNbO_4$.

Single crystals were grown from congruent melts by the Czochralski method by Brixner at DuPont (*7*). The coupled substitution $Ca^{2+} + Mo^{6+} = Ln^{3+} + Nb^{5+}$ keeps the Ln^{3+} dopant ions in the trivalent state. Our samples contained approximately 1.2 mole% $NdNbO_4$ or $YNbO_4$.

The absorption spectra were recorded on a Perkin–Elmer spectrophotometer. The fluorescence spectra and lifetimes were measured using a pulsed nitrogen laser as an excitation source at $\lambda = 337.1$ nm. The excitation pulse is less than 0.4 nm wide and 10 nsec in duration. The samples were mounted in a cryogenic refrigerator capable of controlling the temperature between 10 and 300 K. The fluorescence was analyzed by a 1-m monochromator, detected by a cooled RCA C31034 photomultiplier tube, averaged by a boxcar integrator triggered by the laser, and displayed on a strip-chart recorder. To investigate the characteristics of host-sensitized energy transfer, time-resolved spectroscopy (TRS) measurements were made by gating the boxcar to

* Permanent address: Applied Solid State Chemistry Laboratory, Faculty of Sciences, Charia Ibn Batota Rabat, Morocco.

0022-4596/87 $3.00

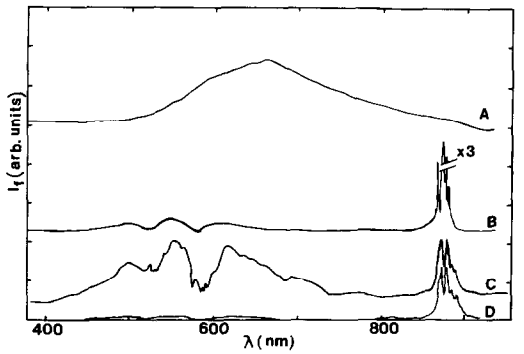

FIG. 1. Examples of fluorescence spectra of some rare earth-doped molybdate crystals. (A) $CaMoO_4$: $YNbO_4$ at 100 μsec after the laser pulse, T = 300 K; (B) $CaMoO_4$: $NdNbO_4$ at 100 μsec after the laser pulse, T = 11 K; (C) $CaMoO_4$: $NdNbO_4$ at 100 nsec after the laser pulse, T = 300 K; (D) $CaMoO_4$: $NdNbO_4$ at 30 μsec after the laser pulse, T = 300 K.

record the spectra at set times after the laser pulse.

II. Experimental Results

The absorption edge of these samples occurs near 340.0 nm, which is similar to undoped $CaMoO_4$ crystals. The temperature and time dependences of the fluorescence emission were studied in detail for both of the samples. Typical examples of the emission spectra taken under different experimental conditions are shown in Fig. 1. $CaMoO_4$: $YNbO_4$ has a broad fluorescence band in the region 400 to 800 nm similar to $CaMoO_4$, except that the emission intensity is stronger and the fluorescence lifetime longer at room temperature than in the undoped material (*1–3*). The structure of this band indicates the presence of two or more unresolved transitions contributing to the observed emission.

The Nd^{3+} absorption transitions in $CaMoO_4$: $NdNbO_4$ are a series of sharp lines associated with $4f$–$4f$ transitions which are similar to Nd^{3+} spectral features in other host crystals. In Fig. 2 the Nd^{3+} emission lines in the visible region of the spectrum associated with the transitions from the $^4F_{3/2}$ metastable state to the crystal field components of the $^4I_{9/2}$ ground state manifold are seen between 850 and 900 nm. These transitions can be used to monitor the fluorescence quenching and energy transfer processes of interest to this study. The Nd^{3+} lines dominate the spectrum observed at 30 μsec after the excitation pulse, whereas the spectrum taken at 100 nsec after the laser pulse also shows the broad emission band of the host crystal. In this case the host emission band exhibits significant structure associated with radiative reabsorption of the fluorescence by the Nd^{3+} ions. The ratio of the integrated areas of the dips in the band caused by radiative energy transfer to that of the total band was found to remain constant at a value of about 0.2 with time after the excitation pulse for all temperatures. This is discussed further in the following section.

The temperature dependences of the fluorescence lifetimes of the host emission

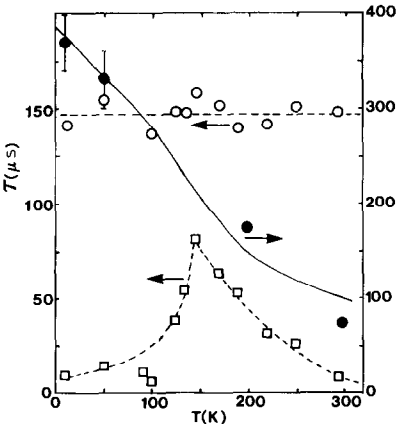

FIG. 2. Temperature dependence of the fluorescence lifetimes of $CaMoO_4$: $YNbO_4$ (solid circles), $CaMoO_4$: $NdNbO_4$ host emission (squares), and Nd^{3+} emission (open circles).

in both the $YNbO_4$- (τ_H°) and $NdNbO_4$- (τ_H) doped samples, and the Nd^{3+} emission (τ_A) in the latter sample, are shown in Fig. 2. τ_H° exhibits a significant decrease between 10 K and room temperature. The spread in data points at low temperature is associated with different values measured at different spectral positions across the broad emission band. This may be attributed to the effects of inhomogeneous broadening at low temperatures due to local disorder in the crystal. Phonon processes cause homogeneous broadening to dominate at high temperatures and a single lifetime is measured for all positions in the band. The temperature dependence of the host fluorescence lifetime in the $NdNbO_4$-doped sample is significantly different from that of the $YNbO_4$ sample, and the magnitude of τ_H is less than that of τ_H° at all temperatures. τ_H increases between 10 and 145 K and then decreases as temperature is raised to 300 K. These characteristics are the effects of host-sensitized energy transfer as well as the presence of thermal quenching, and are discussed further in the following section. The Nd^{3+} fluorescence lifetime is about 148 μsec at all temperatures, which is close to the radiative decay time of 152 μsec predicted by earlier measurements (*8*).

Figure 3 shows the temperature dependences of the fluorescence intensities of the host and Nd^{3+} emission bands in both the $YNbO_4$- and $NdNbO_4$-doped samples. The peaks of the host emission bands in both samples are normalized to a value of 10 at 300 K. These peak intensities generally decrease exponentially as temperature is lowered. The rate of decrease is greater for the host peak in the $NdNbO_4$-doped sample, which exhibits a slight initial increase as temperature is lowered from 300 K and then tends to become constant below 100 K. The integrated intensity of the Nd^{3+} fluorescence near 875 nm also decreases exponentially with decreasing temperature down to about 100 K and then tends toward a constant value. The ratio of the integrated intensities of the Nd^{3+} emission and the host emission in the $CaMoO_4$: $NdNbO_4$ sample is constant between about 50 and 150 K and then decreases exponentially as temperature is increased to 300 K.

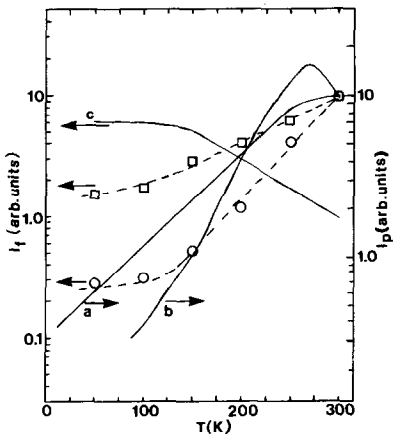

FIG. 3. Temperature dependences of the peak fluorescence intensities of (a) $CaMoO_4$: $YNbO_4$ and (b) $CaMoO_4$: $NdNbO_4$ host emission, the integrated fluorescence intensities of $CaMoO_4$: $NdNbO_4$ host emission (circles) and Nd^{3+} emission (squares), and the ratios of the integrated fluorescence intensities of the Nd^{3+} and host emission in $CaMoO_4$: $NdNbO_4$ (c).

III. Interpretation of Results

The independence of the absorption band edge on doping compositions has been observed previously (*1*, *9*). The band edge absorption has been attributed to a charge transfer transition in which an oxygen $2p$ electron goes into one of the empty $4d$ orbitals of the molybdenum (*9*). The host emission band is associated with the Stokes shifted reverse of this transition. For the samples investigated here, the large spectral shift and long low-temperature lifetime suggest the presence of radiationless relaxation to a triplet excited state before a spin forbidden radiative emission to the singlet ground state (*10*).

The fact that the peak fluorescence intensity of the host emission band in $CaMoO_4:YNbO_4$ increases while the fluorescence lifetime decreases with increasing temperature indicates that thermal processes enhance the radiative emission. A comparison of these results with those published previously (*1*) for $CaMoO_4$ shows that the presence of $YNbO_4$ enhances the room-temperature luminescence. The mechanism for thermal quenching of the luminescence in the similar materials of $CaWO_4$ and YVO_4 has been identified as thermally activated migration of the excitation energy to quenching centers (*11–13*). The introduction of defects into the host crystal can either enhance the quenching if the defects act as additional quenching centers or decrease the quenching if the defects act as scattering or recombination centers to inhibit the exciton migration. If this model is valid for $CaMoO_4$, the presence of $YNbO_4$ appears to introduce recombination centers which cause the mobile excitons to have a higher radiative decay rate than the self-trapped excitons.

The temperature dependences of the fluorescence intensity and lifetime of the $CaMoO_4:YNbO_4$ sample can be attributed to the emission from both free and self-trapped excitons with a thermal equilibrium distribution of the relative population of the two states. These are described by the expressions

$$\tau^{-1}(T) = \tau_t^{-1} + \tau_f^{-1} \exp(-\Delta E/kT) \quad (1)$$

$$I(T) = I_t + I_f \exp(-\Delta E/kT), \quad (2)$$

where k is Boltzmann's constant and ΔE is the activation energy between the free and mobile exciton states. The solid lines in Fig. 2 and curve (a) of Fig. 3 represent the best fits to the data using these equations and treating the activation energy and the free exciton lifetime (τ_f) and emission intensity (I_f) as adjustable parameters. The values giving the best fits are $\Delta E = 212.7$ cm^{-1}, $\tau_f = 50$ μsec, and $I_f = 17.9$. The values used for the trapped exciton lifetime (τ_t) and intensity (I_t) are found from extrapolating the experimental data to zero temperature.

Investigating the characteristics of energy transfer from the host crystal to an optically active impurity ion such as Nd^{3+} can provide further insight into the host energy migration and quenching processes. For $CaMoO_4:NdNbO_4$, host-sensitized energy transfer can take place both radiatively and nonradiatively. The contributions due to these two processes can be separated through their different effects on the host fluorescence properties. Radiative reabsorption does not change the observed lifetime of the host fluorescence while radiationless energy transfer produces lifetime quenching. In addition, the measurements of the structure in the host emission band due to reabsorption show that the radiative energy transfer contribution is independent of temperature and time after the excitation pulse. Radiationless energy transfer varies with both parameters. Our main interest here is understanding the mechanism of radiationless energy transfer and the following discussion deals only with this contribution to the total energy transfer.

The temperature variation of the fluorescence intensity ratios shown in Fig. 3 indicates a constant efficiency for host-sensitized energy transfer between 50 and 150 K, and then a decrease in transfer efficiency as temperature is raised to 300 K. The rate of energy transfer can be defined from the expression

$$\omega = \tau_H^{-1} - (\tau_H^{\circ})^{-1}. \quad (3)$$

The values of ω obtained from the lifetime measurements are plotted versus T^{-1} in Fig. 4. Between 10 and 150 K, the energy transfer rate decreases, and then it increases as temperature is raised to 300 K.

Although both the transfer efficiency and

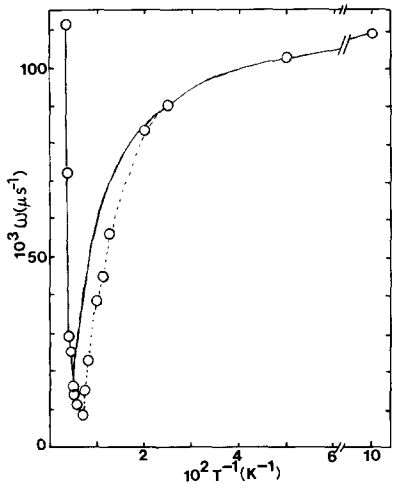

FIG. 4. Temperature dependence of the host-sensitized energy transfer rate. Circles with the dashed line represent values obtained from lifetime quenching measurements and the solid line is obtained from the results of TRS measurements.

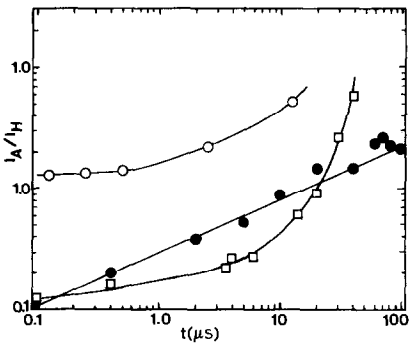

FIG. 5. Time evolution of the integrated fluorescence intensity ratios of the Nd^{3+} and host emission in $CaMoO_4$: $NdNbO_4$ at 10 K. (open circles), 170 K (solid circles), and 300 K (squares). (See text for explanation of theoretical lines.)

transfer rate show changes in their properties at $T = 150$ K, they appear to give contradictory information about the temperature variation of the host-sensitized energy transfer. We attempted to resolve this apparent discrepancy through time-resolved spectroscopy measurements. The fluorescence spectra shown at two times after the laser pulse in Fig. 1 demonstrates the time dependence of the energy transfer from the host to the Nd^{3+} ions. The time evolution of this energy transfer was obtained at numerous temperatures by measuring the fluorescence spectra at many different times after the excitation pulse. Figure 5 shows examples of the time variation of the ratios of the integrated fluorescence intensities of the Nd^{3+} and host emission bands at several temperatures.

Different models were required to obtain the best fits to the TRS data at high and low temperatures. Above 200 K the rate equation model shown in Fig. 6 was used. n_H and n_A represent the concentrations of excited states of the host and Nd^{3+} activator ions, respectively, while β_H and β_A are their fluorescence decay rates. W_H and W_A are the direct pumping rates of the host and activators. The latter will include any excitation of the Nd^{3+} ions due to radiative energy transfer. ω and ω' are the energy transfer and back transfer rates, which for this model are taken to be time independent. The rate equations for the excited state populations are given by

$$dn_H/dt = W_H - \beta_H n_H - \omega n_H + \omega' n_A \quad (4)$$

$$dn_A/dt = W_A - \beta_A n_A + \omega n_A - \omega' n_A. \quad (5)$$

Solving these equations for a delta function excitation pulse gives the ratio of the excited state populations which is related to

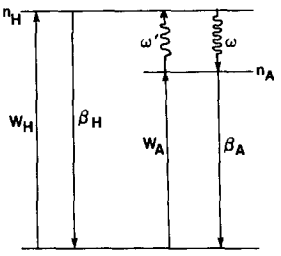

FIG. 6. Energy levels and rate parameters for interpreting host-sensitized energy transfer in $CaMoO_4$: $NdNbO_4$. (See text for explanation of notation.)

the observed ratio of the fluorescence intensities through a factor of the ratio of the radiative decay rates, β_A^r/β_H^r,

$$I_A(t)/I_H(t) = [I_A(0)/I_H(0)] \{[1 + G_1 \tanh(Bt)]/[1 + G_2 \tanh(Bt)]\}, \quad (6)$$

where

$$B = \{[(\omega + \beta_H - \omega' - \beta_A)/2]^2 + \omega\omega'\}^{1/2}$$

$$G_1 = \{[n_H(0)/n_A(0)]\omega + [\omega + \beta_H - \omega' - \beta_A]/2\}/B$$

$$G_2 = \{[n_A(0)/n_H(0)]\omega' - [\omega + \beta_H - \omega' - \beta_A]/2\}/B.$$

An example of the best fit to the data obtained using this equation and treating the initial intensity ratio, energy transfer, and back transfer rates as adjustable parameters can be seen by the solid line in Fig. 5. The parameters giving the best fits to the data at different temperatures are listed in Table I. The ratio of the radiative decay rates is approximated by the ratio of the measured fluorescence decay rates extrapolated to 0 K.

At temperatures of 150 K and less, the same general model shown in Fig. 6 can be used to interpret the TRS data, but the back transfer rate is zero and the energy transfer rate is time dependent. Solving the rate equations under these conditions leads to the expression (*4*)

$$I_A(t)/I_H(t) = \{[I_A(0)/I_H(0)] + 1\} \exp(\omega t^{3/q})^{-1}, \quad (7)$$

where $q = 6$, 8, or 10 for electric dipole–dipole, dipole–quadrupole, or quadrupole–quadrupole interaction. Examples of the best fits to the TRS data are shown as solid lines in Fig. 5 and the parameters needed to obtain the best fits for each temperature are listed in Table I.

The values obtained for ω from fitting the TRS data are used to plot the solid line in Fig. 4 for the purpose of comparing these results with the values of ω obtained from the lifetime quenching measurements.

TABLE I

ENERGY TRANSFER PARAMETERS FOR $CaMoO_4 : NdNbO_4$

T (K)	Model	$I_A(0)/I_H(0)$	ω (μsec^{-1})	ω' (μsec^{-1})	ω (from τ_H) (μsec^{-1})
295	Eq. (6)	0.140	0.1109	0.0382	0.1109
275	Eq. (6)	0.185	0.0722	0.0248	0.0722
250	Eq. (6)	0.280	0.0577	0.0	0.0290
220	Eq. (6)	0.400	0.0619	0.0	0.0249
190	Eq. (7), $q = 8$	0.000	0.0408[a]	0.0	0.0136
170	Eq. (7), $q = 8$	0.000	0.0490[a]	0.0	0.0111
100	Eq. (7), $q = 10$	0.200	0.0662[a]	0.0	0.0383
90	Eq. (7), $q = 10$	0.720	0.0662[a]	0.0	0.0445
10	Eq. (7), $q = 10$	0.400	0.1069[a]	0.0	0.1083

[a] At $t = 15$ μsec.

Since the TRS analysis gives a time-dependent energy transfer rate in the low-temperature region, the values listed in Table I and plotted in Fig. 5 are for a specific time after the excitation pulse. For the purpose of this comparison we have chosen the values at 15 μsec. The general shapes of the curves of ω versus T obtained from the two different types of measurements are similar and show a distinct change in properties near 150 K. At the highest and lowest temperatures the magnitudes of ω obtained by the two methods are very similar, while at intermediate temperatures the values of ω obtained from TRS measurements are larger than those obtained from lifetime quenching measurements.

IV. Conclusions

The results reported here show that efficient host-sensitized energy transfer takes place in $CaMoO_4 : NdNbO_4$. At low temperatures the characteristics of the transfer process are consistent with a single-step, multipole–multipole interaction mechanism. The rate of this process decreases as temperature is raised while the total amount of energy transfer remains constant. This is consistent with transfer from

localized excited states of MoO_4^{2-} molecular ions to their nearest-neighbor Nd^{3+} ions, with a statistical distribution of transfer distances. Increasing temperature causes the energy transfer to occur with a smaller rate but allows the same total amount of transfer to occur. This can be explained if the laser is preferentially exciting MoO_4^{2-} ions near Nd^{3+} ions. This is very probably the case since the laser excitation at 337.1 nm is just higher than the band edge of 340.0 nm, and it has been shown for other materials that excitation into the "red edge" of the host band preferentially excites regions of the host crystal near defects (*12, 14*). If there are extended trapping regions around each activator, increasing the temperature will allow excitons in the outer regions of the trap to migrate closer to the Nd^{3+} before transfer occurs.

At very high temperatures the host-sensitized energy transfer characteristics are consistent with a multistep energy migration process in which the energy migrates among several MoO_4^{2-} ions before transferring to a Nd^{3+} ion. This thermally activated exciton model has been used to characterize host-sensitized energy transfer in similar crystals (*11–13*). As temperature is raised in this range, the transfer rate increases while the total amount of transfer decreases. This indicates that the excitons have become mobile enough to migrate away from the Nd^{3+} trapping regions. As the rate of migration increases with temperature, the rate of energy transfer to Nd^{3+} ions will increase but the rate of interaction with other trapping centers will also increase, thus decreasing the total amount of energy transfer to Nd^{3+} ions.

The energy transfer characteristics in the Nd^{3+}-activated crystal indicate that thermally activated energy migration may be responsible for the quenching of luminescence in molybdate crystals. Then doping with $YNbO_4$, which is not optically active, can enhance the room-temperature luminescence of the host by providing recombination centers for the migrating excitons. The room-temperature quantum efficiency of the $CaMoO_4$:$YNbO_4$ crystal investigated here was approximately 18%. Although this is not high, it appears that this type of mixed crystal might be usable for broadband tunable laser applications. The efficient host-sensitized energy transfer observed here along with the optically pumped laser properties of $CaMoO_4$:Nd NbO_4 reported previously (*4, 6*) indicates that this type of mixed crystal may be a good laser material for nitrogen or eximer laser pumping.

Acknowledgments

This work was sponsored by the U.S. Army Research Office. The crystals were supplied by L. H. Brixner of DuPont.

References

1. F. A. KROGER, "Some Aspects of Luminescence of Solids," Elsevier, Amsterdam (1948).
2. G. BLASSE AND G. D. M. VAN DEN HEUVEL, *J. Lumin.* **9,** 74 (1974).
3. J. A. GROENINK, C. HAKFOORT, AND G. BLASSE, *Phys. Status Solidi A* **54,** 477 (1979).
4. R. C. DUNCAN, *J. Appl. Phys.* **36,** 874 (1965).
5. L. F. JOHNSON, G. D. BOYD, K. NASSAU, AND R. R. SODEN, *Phys. Rev.* **126,** 1406 (1962).
6. P. A. FLOURNOY AND L. H. BRIXNER, *J. Electrochem. Soc.* **112,** 779 (1965).
7. L. H. BRIXNER, *J. Electrochem. Soc.* **111,** 690 (1964); **113,** 621 (1966); and **114,** 108 (1967).
8. T. S. LOMHEIM AND L. G. DESHAZER, *J. Appl. Phys.* **49,** 5517 (1978).
9. G. BLASSE, *Structure and Bonding* **42,** 1 (1980).
10. C. J. M. COREMANS, J. H. VAN DER WAALS, J. KONIJNENBERG, A. H. HUIZER, AND C. A. G. O. VARMA, *Chem. Phys. Lett.* **125,** 514 (1986).
11. M. J. TREADAWAY AND R. C. POWELL, *Phys. Rev. B* **11,** 862 (1975); *J. Chem. Phys.* **61,** 4003 (1974).
12. R. C. POWELL AND G. BLASSE, *Structure and Bonding* **42,** 63 (1980).
13. C. HSU AND R. C. POWELL, *J. Lumin.* **10,** 273 (1975); D. K. SARDAR AND R. C. POWELL, *J. Appl. Phys.* **51,** 2829 (1980).
14. R. G. PETERSON AND R. C. POWELL, *J. Lumin.* **16,** 285 (1978).